An Experimental and Numerical Analysis of the Flexural Performance of Lightweight Concrete Beams reinforced with GFRP Bars

Mohamed A. El Zareef
Civil Engineering Department, College of Engineering and Islamic Architecture, Umm Al-Qura University, Saudi Arabia | Structural Engineering Department, Faculty of Engineering, Mansoura University, Egypt
mazareef@uqu.edu.sa (corresponding author)

Received: 21 March 2023 | Revised: 30 March 2023 | Accepted: 3 April 2023

 DOI: https://doi.org/10.48084/etasr.5871

ABSTRACT

Occasionally it is more crucial to lower the mass of a building component than to improve its rigidity, specifically in massive buildings like long-span structures where the self-weight of the floors is one of the significant challenges that engineers confront. Therefore, the main objective of this work is to explore the flexural performance of Lightweight Concrete Beams (LWCBs) reinforced with Glass Fiber Reinforced Polymer (GFRP) bars in terms of curvature, cracks and failure modes, deflection, material stress-strain relationship, and joint end rotation. The flexural performance of LWCBs reinforced with varied GFRP bars and Steel Reinforcement (SR) ratios is assessed and compared to that of Normal Concrete Beams (NCBs) reinforced with SR. Numerical analytical models for the tested beams were created utilizing the iDiana software. Both analytical and experimental test results were compared. The study revealed a high correlation between the findings of Finite Element Models (FEMs) and those acquired from beam testing. The performance of LWCBs that utilized SR was equivalent to that of NCBs. The GFRP-reinforced LWCBs performed mostly as elastic deformed elements, with just little deflection post-load release. The study emphasized the significant potential for employing LWC and GFRP bars in the construction field's growth.

Keywords-flexural behavior; LWC beams; GFRP bars; FEM of LWC beams

I. INTRODUCTION

The analysis of prior research indicates that there are few available experimental tests for the bending response of beams made of LWCBs reinforced with GFRP bars, particularly for LWC beams with a specific gravity half that of NC. Many of these researches [1-12] were concerned with the structural behavior and the mechanical characteristics affected by the type of Lightweight Aggregates (LWA) and the composition of the LWC blends as well as the kind and ratio of Fiber Reinforced Polymer (FRP) reinforcement. Authors in [1] experimentally tested lightweight and fibered lightweight concrete (LWC and LWCF) beams in terms of bending and ductility and compared the results with that of conventional concrete beams. They stated that the LWC beams exhibited significantly better performance than that of LWCF beams. A 16% reduction was observed in the weight of LWCF beams. The ductility was improved by 0.4% and 0.5% for LWC and LWCF beams, respectively. Authors in [2] conducted a series of experimental tests to explore the properties of LWC blends using Expanded Polystyrene Beads (EPBs) instead of Coarse Aggregates (CA). The study concluded that adding EPB as a replacement of CA declined the mixes' density to 10.9KN/m^3, resulting in reducing the concrete compression capacity and modules of rupture. Authors in [3] studied the structural performance of a LWC beam reinforced with glass-and basalt-reinforced polymer (GFRP and BFRP) bars. The LWC in the study was created by replacing 50% of the normal aggregates with expanded clay LWA. According to that study, increasing the percentage of expanded clay LWA in concrete lowered its compressive strength. The ultimate load capacity and mid-span deflection for GFRP and BFRP reinforced beams were lower than those of steel-reinforced beams. Authors in [4] investigated the deflection of six steel-fibered LWC beams reinforced with Carbon-FRP (CFRP) rods under two-point loads. The testing results demonstrated that the introduction of steel fibers at a ratio of 0.6% by volume enhanced the structural behavior of the beams in bending, resulting in a 30% reduction in maximum deflection when compared to LWC beams without steel fibers. The maximum deflection of the LWC beams reinforced with CFRP rods was less than the permitted limit specified by ACI code requirements.

The goal of the current experimental and numerical analysis is to explore the performance of RC-beams made of LWC, which has a specific gravity half that of normal concrete and cylinder compressive strength of 30MPa. The LWC beams were reinforced with varied ratios of GFRP and SR rods. Four

LWC beams were assessed in terms of bending performance, failure mode, and serviceability, in addition to two reference beams built of NC with cylinder compressive strength of 30MPa.

II. CHARACTERISTICS OF MATERIALS UTILIZED IN BEAM PRODUCTION

A. Glass Fiber Reinforced Polymer and Steel Rods

One downside of utilizing SR in structural concrete is the likelihood of corrosion, particularly in settings with high humidity and chloride attack. One good remedy for this issue is to use GFRP bars in reinforcing structural elements instead of SR bars since they are non-corroded. The axial and lateral resistance of the GFRP rods is regulated by the kind, quantity, and configuration of the GF utilized in each rod. Throughout all loading phases, the GFRP rods acted as a perfectly elastic material. The lateral resistance of GFRP rods is substantially lower than that of SR bars, but it has a higher tensile capacity. Table I and Figure 1 provide the design parameters of the utilized GFRP and SR rods. Figure 2 displays the results of the pull-out test between the LWC utilized in the current research and various reinforcing bars.

TABLE I. CHARACTERISTICS OF GFRP AND SR RODS

Design parameter	GFRP rods	STR rods
Ultimate tension capacity (MPa)	1000	620
Yield strength (design strength) (MPa)	420[a]	420
Elastic modulus (GPa)	60×10^3	200×10^3

[a]. The GFRP rods have design strength and no yielding took place

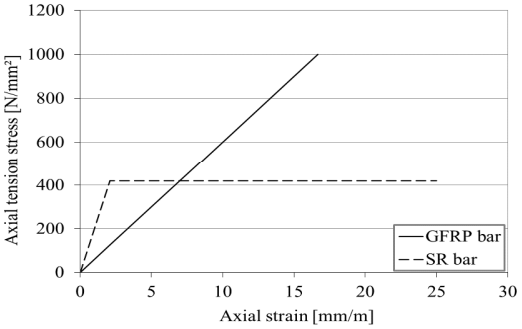

Fig. 1. SR and GFRP bar's stress and strain under tension load.

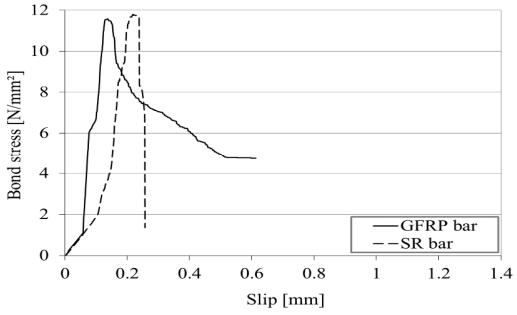

Fig. 2. Relationship of bond stress between LWC and different types of bars.

B. Mechanical Properties of the utilized LWC

LWC is encouraged to be applied in the construction industry due to its favorable physical characteristics, including low heat conductivity and density. The LWC used in the present study was developed to have the half-density of NC [13]. Table II displays the design parameters of the LWC employed in the current research as well as the composition of $1m^3$ expressed as a percentage of cement weight. Figure 3 illustrates the splitting and flexural tensile test for the LWC employed in the study.

TABLE II. LWC BLEND COMPOSITION AND MECHANICAL CHARACTERISTICS

Material/Mechanical properties	Percentage of cement weight / value
Cement type I 52.5	1
Fine expanded clay 0/2	0.83
Coarse expanded clay 2/9E	0.15
Coarse expanded clay 6.5	1.06
Water-cement ratio	0.63
Silica fume	0.08
Super plasticizer	0.01
Concrete compressive strength (MPa)	34
Direct tensile strength (MPa)	2.25
Modulus of rupture (MPa)	2.46
Elastic modulus (GPa)	12×10^3
Fresh/dry specific weight (g/cm^3)	1.43/1.25

(a) (b)

Fig. 3. (a) Splitting and (b) flexural tensile strength tests of the used LWC.

C. Beam Preparation and Test Setup

Four simply supported beams with a reinforcement ratio of 0.5% and 1% were manufactured using LWC, which had a specific gravity half that of NC. Two other beams were built utilizing NC with the same steel reinforcement ratios of 0.5% and 1.0% for comparison. All the tested beams had a 3300mm overall length, 150mm×300mm cross-sectional dimensions, and were exposed to 2-point loads at the third span. All tested beams were subjected to displacement control technique with a loading rate of 0.01mm/s. All beams' longitudinal bars were extended to the beam's end for a total of 3300mm. LVDT gauges were affixed to the ends of the bars at the end face of the beam to measure any slippage between the longitudinal bars and the surrounding concrete at the end zone of the beam. Figure 4 displays the beam dimensions and the test set up. Several methods have been employed to monitor each tested beam. Five different locations underneath each beam were used to detect the deflection using LVDTs. Four 2-gauge LVDTs at the ends of the beams were used to keep record of the slippage between the longitudinal compression of tensile reinforced bars and concrete. The gauges were used to quantify the compressive and tension strains in the horizontal and vertical bars. The gauges were affixed to the beam surface 20mm in the compression area, to determine the height of the compression side at the beam's mid-span. With the help of the iDiana FE software, the gauge locations were established.

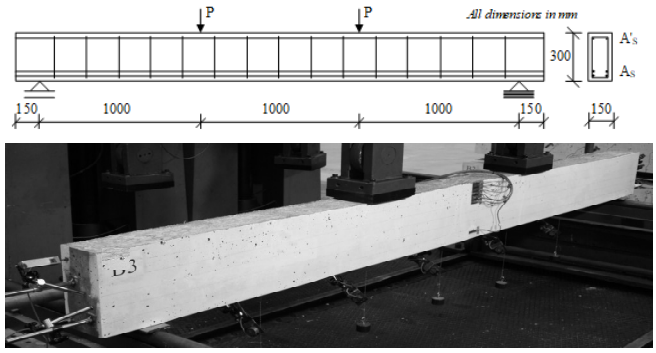

Fig. 4. Dimensions and test setup for the tested beams.

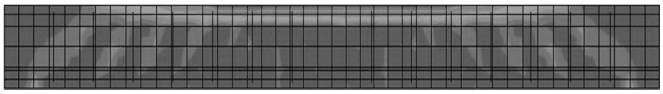

Fig. 5. FEM of the S1 tested beam.

In order to design the examined beams in accordance with ACI 440.1R-15 [14], and to look into model expectations for the behavior of the beams, such as the moment-curvature relationship and the transmission of stresses and strains throughout the beams, the FE model depicted in Figure 5 was created using the iDiana software prior to the conducted experiments. Table III displays the beams' details.

TABLE III. FEATURES AND DETAILS OF THE STUDIED BEAMS

Beam ID	S1	S2	S3	S4	S5	S6
Concrete type	LWC	LWC	LWC	LWC	NC	NC
Concrete grade (MPa)	30/33	30/33	30/33	30/33	30/37	30/37
Cross-section (mm)	150×300					
Bar type	GFRP	GFRP	SR	SR	SR	SR
Reinforcement ratio (%)	1.0	0.5	1.0	0.5	1.0	0.5
Top reinforcement	2 φ 8					
Transverse reinforcement/m	10 φ 8					

III. FINITE ELEMENT MODEL VALIDATION

The moment-curvature relationships produced by the developed FEM were compared with those established based on the experimental data. By dividing the maximum compression strain at the topmost layer of the beam by the height of the compression zone, it is possible to compute the curvature at various bending moment values. Using 6 strain gauges, each 20mm in the mid-span compression zone, it was possible to experimentally measure both the maximum compression strain and the depth of the compression zone as depicted in Figure 4. The moment-curvature relationships produced by the FEM and the experimentally tested beams are displayed in Figure 6. Two sets of beams were considered with regard to reinforcing ratio. The reinforcement ratio for sets S1, S3, and S5 was 1% and 0.5% for S2, S4, and S6. Apart from B1, LWC beams reinforced with GFRP bars with 1% reinforcement ratio, there is generally no discernible variation between the numerical and the test-generated moment-curvatures. In B1, the variation in curvature between the experimental and FEM curves reaches 25.2% at the breakdown. The response of LWC beams reinforced with SR rods is comparable to that of NC beams, particularly at small reinforcement ratios. Nevertheless, utilizing GFRP rods boosts the LWC beams' curvature at the same load level. It should be mentioned that the moment capacity of the SR beams (LWC or NC beams) reaches a specific level and is maintained for a considerable rise in curvature prior to the collapse. The GFRP-reinforced beams can, however, reveal deformation features similar to those of SR-reinforced beams before failure. The major distinction is that they have no ability to retain maximum moments with extended curvature before failure. This may be explained by the fully elastic properties of GFRP bars and the elastoplastic response of SR bars.

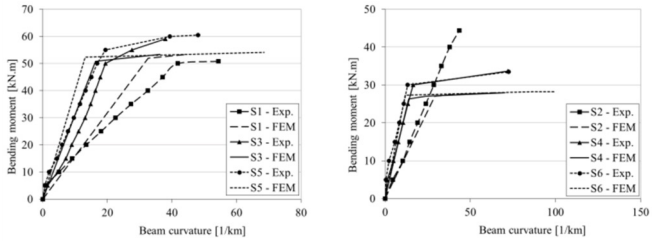

(a) (b)

Fig. 6. Moment-curvature relationship of the experimentally tested beams and FE models at (a) 1% and (b) 0.5% reinforcement ratio.

IV. END-ROTATION RESPONSE OF THE STUDIED BEAMS

The moment end-rotation relationships for SR- and GFRP-reinforced LWC and NC beams are shown in Figure 7. The end-rotation might be computed at every load stage until the beam failure since the deflection readings at 0.5m from the support point throughout each beam's test have been recorded. The findings demonstrate that the moment-end rotation relationship for NC and LWC samples reinforced with SR bars are fairly similar. The geometry of the moment end-rotation relationship for SR-reinforced LWC and NC samples complies with the typical tendency of a moment-curvature relationship, increasing linearly till the yield of the SR bars. When the SR bars yielded, that caused a significant rise in end-rotation with a small raise in the bending moment, particularly when the reinforcement ratio was small, as in samples S4 and S6. This response indicates that the rotation-ductility of LWC and NC beams reinforced with SR bars is extremely similar.

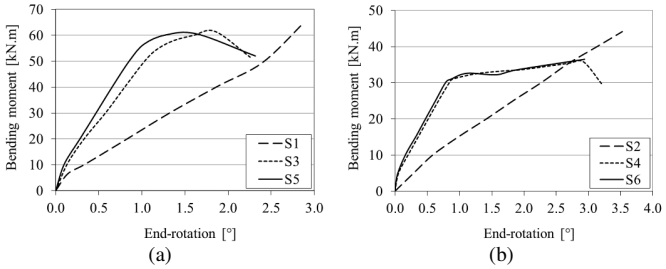

(a) (b)

Fig. 7. Moment end-rotation relationship of the studied beams with (a) 1% and (b) 0.5% reinforcement ratio.

It was noticed that the end-rotation of these samples immediately before rupture differed between 2°17' and 3°14' based on the ratios of reinforced bars. The moment end-rotation relationships for GFRP-reinforced LWC samples rise linearly until the rupture point. The greatest end-rotation for GFRP-reinforced samples ranged between 2°51' and 3°31', exceeding the greatest end-rotation for SR-reinforced beams. Generally, the bar's modulus of elasticity has a substantial effect on the moment end-rotation relationship.

V. LOAD-DEFLECTION RELATIONSHIP

Figure 8 depicts the load-deflection curves for the investigated beam sets (S1, S3, and S5) and (S2, S4, and S6). The LWC samples reinforced with SR bars (S3 and S4) performed similarly to the NC reference samples (S5 and S6). As predicted, the SR-reinforced LWC and NC samples turned nonlinear following the yielding of SR bars, with a dramatic rise in deflection, but a minimal rise in load capacity. Nevertheless, the GF-reinforced samples functioned in a different way. The load increased with deflection, and the load-deflection curve was nearly linear until rupture.

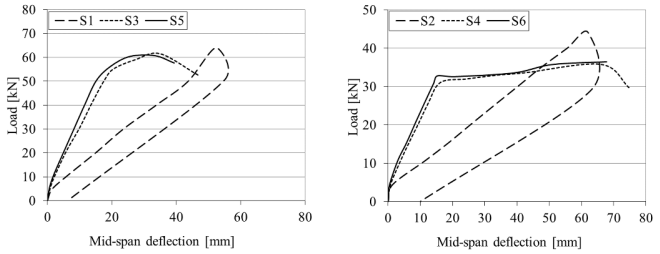

Fig. 8. Load-deflection curves of the studied beams reinforced with (a) 1% and (b) 0.5% reinforcement ratio.

Prior to the SR yield, the maximum deflections of GF-reinforced samples were 3 times greater than those of SR-reinforced samples. SR-reinforced samples with a 0.5% reinforcement ratio (S4 and S6) exhibit better ductile responses than those with a 1% reinforcement ratio (S3 and S5) at the maximum load phase. The mid-span deflection of the GF-reinforced sample (S1) was 1.5-times greater than those of the SR-reinforced samples (S3 and S5) for 1% reinforcement ratio, while for samples with 0.5% reinforcement ratio, the mid-span deflection in the GF-reinforced beam (S2) was nearly equivalent to those of the SR-reinforced samples (S4 and S6). For higher reinforcement ratios, the discrepancy in mid-span deflection between GF- and SR-reinforced samples is greater than at small reinforcement ratios.

VI. CRACK NUMBER AND DISTANCE

The number of cracks and the distance between them, at different load stages, were recorded for all tested beams. Table IV summarizes the crack behavior of the LWC and NC beams at various reinforcing ratios. The tested beams' side area was partitioned into 3 equal portions (2 outer areas and 1 central area). The number and distance between cracks were measured in each of these areas right before the beam's ultimate strength. For the reference beams made of NC and reinforced with SR bars, the number of cracks in the lower 3-quarters of the height of the central area ranged between 11 and 13, with a maximum spacing between cracks ranging from 91 to 111mm. The lower number of cracks (11:13) compared to (27:39) for GF-reinforced beams (S1 and S2) may be due to the lower modulus of elasticity of GFRP bars compared to SR bars. The height of cracks up to 3-quarters of the height of the reference beams revealed a typical tension failure mode for SR-reinforced beams.

When considering the GFRP reinforcement ratio, the frequency of cracks tended to raise with low reinforcement ratios. These findings may represent the impact of bar diameter and rib count on GFRP bars in enhancing bond and crack behavior, as reported in [15, 16]. The crack spacing for SR-reinforced beams made of NC is larger than that of beams made of LWC. This might imply that the bond and tensile strengths of NC are somewhat greater than those of LWC. Another observation made during tests is that cracks in SR-reinforced NC and LWC beams migrated upward with steady rise in point loads. But, in GFRP-reinforced beams, cracks grew swiftly from the bottom edge up to an altitude of three-quarters of the entire height, after which the cracks did not proceed further until collapse. This allows GFR rods with high strains to create the needed stresses to maintain force balance and reveals the impact of GFR rods with low modulus of elasticity.

TABLE IV. DETECTED CRACK NUMBER AND DISTANCE

Beam ID	Ultimate load[a] (kN)	Crack spacing (mm)	Number of cracks			Failure succession	
			Left area	Central area	Right area	First	Final stage
S1	64.1	36	22	27	21	GFRP[b] design strength 420MPa	Crushing in compression zone
S2	44.07	31	28	39	30		
S3	61.55	61	12	21	13	Yield of SR bars	
S4	35.81	66	10	17	13		
S5	60.79	91	10	13	9		
S6	36.44	111	8	11	8		

[a]. The ultimate load value represents the value of load at each point on the beam

[b]. GFRP bars have a perfect linear-elastic response with no yielding until rupture at 1000MPa

VII. CONCLUSIONS

Based on the outcomes of the current research, the following conclusions can be drawn:

- To present the LWC and NC beams reinforced with GFRP and SR bars, FEMs were created and verified after the comparison with the experimental results.
- In terms of maximum load capacity, moment-curvature, deflection, end-rotation, crack behavior, and failure mode, LWC and NC beams reinforced with SR bars displayed to a great extent an equivalent flexural performance.
- The beams reinforced with GFRP bars had a similar load capacity, but a larger deflection than those strengthened with SR bars. This might be ascribed to the lower Young's modulus of GFRP bars.

- Following load discharge, the remnant deformations in GFRP-reinforced beams may be ignored in comparison to those in SR-reinforced beams. This might allude to the GFRP bars' perfect linear-elastic behavior as opposed to the SR bars' elastoplastic behavior.
- The progression of crack height in GFRP-reinforced beams is quicker in the early stages of loading until it reaches around three-quarters of the beam's height and then becomes significantly slower until failure.
- The progression of fracture height in SR-reinforced beams behaved gradually as applied loads increased.

REFERENCES

[1] Z. H. Dakhel and S. D. Mohammed, "Castellated Beams with Fiber-Reinforced Lightweight Concrete Deck Slab as a Modified Choice for Composite Steel-Concrete Beams Affected by Harmonic Load," *Engineering, Technology & Applied Science Research*, vol. 12, no. 4, pp. 8809–8816, Aug. 2022, https://doi.org/10.48084/etasr.4987.

[2] A. S. Salahaldeen and A. I. Al-Hadithi, "The Effect of Adding Expanded Polystyrene Beads (EPS) on the Hardened Properties of Concrete," *Engineering, Technology & Applied Science Research*, vol. 12, no. 6, pp. 9692–9696, Dec. 2022, https://doi.org/10.48084/etasr.5278.

[3] M. A. Abed, A. Anagreh, N. Tošić, O. Alkhabbaz, M. E. Alshwaiki, and R. Černý, "Structural Performance of Lightweight Aggregate Concrete Reinforced by Glass or Basalt Fiber Reinforced Polymer Bars," *Polymers*, vol. 14, no. 11, Jan. 2022, Art. no. 2142, https://doi.org/10.3390/polym14112142.

[4] Y. Sun, T. Wu, and X. Liu, "Serviceability performance of fiber-reinforced lightweight aggregate concrete beams with CFRP bars," *Advances in Structural Engineering*, vol. 25, no. 1, pp. 117–132, Jan. 2022, https://doi.org/10.1177/13694332211043333.

[5] S. Mehany and H. M. Mohamed, "Innovative Lightweight Concrete (LWC) for Precast Structures," in *2022 ASU International Conference in Emerging Technologies for Sustainability and Intelligent Systems (ICETSIS)*, Manama, Bahrain, Jun. 2022, pp. 285–288, https://doi.org/10.1109/ICETSIS55481.2022.9888931.

[6] A. W. Ali and N. M. Fawzi, "Production of Light Weight Foam Concrete with Sustainable Materials," *Engineering, Technology & Applied Science Research*, vol. 11, no. 5, pp. 7647–7652, Oct. 2021, https://doi.org/10.48084/etasr.4377.

[7] N. A. Memon, M. A. Memon, N. A. Lakho, F. A. Memon, M. A. Keerio, and A. N. Memon, "A Review on Self Compacting Concrete with Cementitious Materials and Fibers," *Engineering, Technology & Applied Science Research*, vol. 8, no. 3, pp. 2969–2974, Jun. 2018, https://doi.org/10.48084/etasr.2006.

[8] Z. A. Tunio, B. A. Memon, N. A. Memon, N. A. Lakho, M. Oad, and A. H. Buller, "Effect of Coarse Aggregate Gradation and Water-Cement Ratio on Unit Weight and Compressive Strength of No-fines Concrete," *Engineering, Technology & Applied Science Research*, vol. 9, no. 1, pp. 3786–3789, Feb. 2019, https://doi.org/10.48084/etasr.2509.

[9] Y. Yuan, Z. Wang, and D. Wang, "Shear behavior of concrete beams reinforced with closed-type winding glass fiber-reinforced polymer stirrups," *Advances in Structural Engineering*, vol. 25, no. 12, pp. 2577–2589, Sep. 2022, https://doi.org/10.1177/13694332221104280.

[10] S. A. Mohammed and A. I. Said, "Analysis of concrete beams reinforced by GFRP bars with varying parameters," *Journal of the Mechanical Behavior of Materials*, vol. 31, no. 1, pp. 767–774, Jan. 2022, https://doi.org/10.1515/jmbm-2022-0068.

[11] S. Mehany, H. M. Mohamed, and B. Benmokrane, "Flexural Strength and Serviceability of GFRP-Reinforced Lightweight Self-Consolidating Concrete Beams," *Journal of Composites for Construction*, vol. 26, no. 3, Jun. 2022, Art. no. 04022020, https://doi.org/10.1061/(ASCE)CC.1943-5614.0001208.

[12] S. Mehany, H. M. Mohamed, and B. Benmokrane, "Performance of Lightweight Self-Consolidating Concrete Beams Reinforced with Glass Fiber-Reinforced Polymer Bars without Stirrups under Shear," *Structural Journal*, vol. 120, no. 1, pp. 17–30, Jan. 2023, https://doi.org/10.14359/51737229.

[13] M. A. M. E. Zareef, "Conceptual and Structural Design of Buildings made of Lightweight and Infra-Lightweight Concrete," Ph.D. dissertation, Technical University Berlin, Berlin, Germany, 2010, https://doi.org/10.14279/depositonce-2415.

[14] ACI Committee 440, "Guide for the Design and Construction of Structural Concrete Reinforced with Fiber-Reinforced Polymer (frp) Bars," American Concrete Institute, Farmington Hills, MI, USA, ACI 440.1R-15, 2015.

[15] M. A. El Zareef, "Seismic damage assessment of multi-story lightweight concrete frame buildings reinforced with glass-fiber rods," *Bulletin of Earthquake Engineering*, vol. 15, no. 4, pp. 1451–1470, Apr. 2017, https://doi.org/10.1007/s10518-016-0027-0.

[16] M. El Zareef and M. Schlaich, "Bond behaviour between GFR bars and infra-lightweight concrete," in *Tailor Made Concrete Structures*, J. C. Walraven and D. Stoelhorst, Eds. London, UK: Taylor & Francis Group, 2008.